Arch. Metall. Mater. **68** (2023), 2, 517-524

DOI: https://doi.org/10.24425/amm.2023.142430

L. KUCHARIKOVÁ[1], L. PASTIEROVIČOVÁ[1*], E. TILLOVÁ[1], M. CHALUPOVÁ[1], D. ZÁVODSKÁ[1,2]

INVESTIGATION OF SELF-HARDENING AlZn10Si8Mg CAST ALLOY FOR THE AUTOMOTIVE INDUSTRY

Self-hardening aluminium alloys represent a new and interesting group of aluminium alloys. They have the advantage that they do not need to be heat treated, which is an important advantage that contributes to a significant reduction in production costs of some components and in the amount of energy used. The present paper deals with the possibility to replace the most used heat treatable AlSi7Mg0.3 cast alloys with a self-hardened AlZn10Si8Mg cast alloy. In this study, microstructural characterization of tensile and fatigue-tested samples has been performed to reveal if this replacement is possible. The results of fatigue tests show that AlSi7Mg0.3 alloy after T6 heat treatment and self-hardened AlZn10Si8Mg has comparable values of fatigue properties. The self-hardening alloy has slightly lower strength, ductility, and hardness.

Keywords: self-hardening alloy; mechanical properties; fatigue; deep-etching; aluminium alloy

1. Introduction

Aluminium has many different applications. In transport, it reduces the carbon footprint of cars and trucks (an average of 140 kg is in every new car). Aluminium is infinitely recyclable. It remains essentially unchanged no matter how many times it is processed and used. Therefore, it can be considered as a material with permanent characteristics, one that is not consumed but used over and over again, without the loss of its essential properties. 75% of all the aluminium ever produced is still in use today. Europe is the world's greatest per capita recycler. Over half of all the aluminium currently produced in the European Union originates from recycled aluminium put on the market by refiners and remelters - and that trend is on the increase [1].

Aluminium production is an energy-intensive process that uses elevated temperatures and has a significant impact on the environment. For this reason, foundries are focusing on minimizing the production of primary aluminium components and replacing them with secondary (recycled) aluminium [2,3]. Secondary aluminum gets its name from its source. It's 'secondary' because it is made from recycled aluminum scrap. This scrap can come from all sorts of aluminum products and profiles, such as aluminum turnings, aluminum sheets, aluminum shreds, aluminum radiators, cast aluminum, extrusions, painted sidings, aluminum dross, and more. Generally, secondary aluminum has a higher tolerance for alloying elements, such as iron, magnesium, and silicon (which are commonly added in the recycling process) [1].

Al-Si alloys are the most representative secondary alloys for foundry applications since they have multiple uses in producing commercial products [4-6]. The automotive and aerospace industries rely heavily on aluminum alloys specifically for fuel efficiency and reduction of emissions since strict environmental requirements. Silicon is known to be an alloying element that provides the alloy with excellent castability and allows perfect reproduction of the mould geometry with a minimal number of casting defects. The combination of other elements in Al-Si alloys, such as Mg, Cu, Mn, Zn, Sr, Ti, and B, is highly used to improve the hardness, fracture toughness, and corrosion resistance, thereby increasing the range of applications of these alloys [4-9]. From the industrial point of view, the commonly used alloy for the production of automobile castings such as cylinder blocks and heads, valve lifters, pistons, and so on, is foundry AlSi7Mg0.3 (A356.0) alloy [10,11]. Properties of conventional AlSi7Mg0.3 alloy are influenced by morphology, shape, and distribution of α(Al)-matrix, Si particles, second phases, and structural defects. The size, shape, and amount of these structural components are affected by chemical composition, melt processing conditions, grain refinement, modification, solidification rate, casting process, heat treatment, etc. [11-13]. In particular, the heat treatment is used to improve the mechanical properties especially yield

[1] UNIVERSITY OF ŽILINA, FACULTY OF MECHANICAL ENGINEERING, DEPARTMENT OF MATERIALS ENGINEERING, UNIVERZITNÁ 8215/1, 010 26 ŽILINA, SLOVAK REPUBLIC
[2] SCHAEFFLER SLOVAKIA, KYSUCKÉ NOVÉ MESTO, SLOVAK REPUBLIC

* Corresponding author: lucia.pastierovicova@fstroj.uniza.sk

strength by promoting the formation of small hard precipitates that prevent the movement of dislocations [12,14].

Precipitation hardening heat treatment is the most used process to achieve the optimal combination of strength and ductility of Al-Si-Mg castings owing to the addition of Mg. Mg increases the strength and hardness of the castings. Strengthening is provided by the formation of Mg_2Si phase precipitates during T6 heat treatment. The alloy has maximum hardness during precipitation of fine, matrix-coherent phases. Additionally, during heat treatment, the eutectic Si undergoes three morphological transformations, changing from fragmentation to spheroidisation to coarsening. Some researchers report that the more spherical the eutectic, the higher the tensile strength and elongation are achieved [11,12]. However, castings produced by this process are affected by some intrinsic defects like gas and shrinkage pores that form during processing, trapped oxide films, and intermetallic phases, which have an unfavorable effect on the mechanical properties, especially fatigue behavior [5,13,15]. On the other hand, self-hardening AlZn10Si8Mg represents an innovative class of lightweight Al-alloy used for the production of castings characterized by satisfying mechanical properties without any heat treatment due to natural ageing at room temperature for 7-10 days. Natural ageing achieves good final mechanical properties without further heat treatment. Therefore, the use of self-hardening alloys can be considered a good choice not only in terms of time-saving but also in terms of energy consumption. The AlZn10Si8Mg alloy is becoming increasingly popular in the automotive industry, where it is used for components working under variable load conditions, replacing the AlSi7Mg alloy previously used for such applications. In general, self-hardening alloys are used wherever castings are expected to perform at high fatigue strengths, which are influenced, by microstructure, non-metallic inclusions, and porosity [2,7,8,11,13,15]. Authors Závodská [2] and Vicen [16] confirmed in their research works the fact the fatigue strength of AlZn10Si8Mg is higher compared to AlSi7Mg0.3 alloy due to the morphology of structural components such as eutectic silicon is in form of isolated rods without any heat treatment or modification. Only porosity had a negative effect on fatigue properties, which initiated the formation of cracks, however, this is common for both secondary alloys. Therefore, from the fatigue results [16] can be concluded that AlZn10Si8Mg alloy is suitable for cyclically loaded components and is a potential alternative for AlSi7Mg0.3 alloy.

In view of the above, the aim of the study presented in this paper is to investigate the possibility of replacing a commonly used secondary cast alloy by a self-hardening alloy in terms of microstructure, mechanical, and fatigue properties.

2. Experimental material

The secondary AlSi7Mg0.3 (EN 42100, A356) and AlZn-10Si8Mg (EN 71 100, UNIFONT®-90) alloys used in this study were cast by gravity method into the sand molds in the form of rods with dimensions of length 300 mm and diameter 20 mm at UNEKO, LtD. A sand mould originates from pouring a self-hardening moulding mixture- siliceous sand, furane resin, hardener, and coated with a protective spray. The AlSi7Mg0.3 alloy was delivered in an as-cast state and after heat treatment according to the T6 method consisting of a solution treatment at 530°C ± 5°C / 7 hours then rapid water quenching to water (50°C) followed by artificial aging at 160°C / 6 hours. The alloy AlZn10Si8Mg was delivered after storage for approximately 10 days at room temperature in order to reach optimal properties. The chemical composition of experimental alloys according to the delivery lists from UNEKO, LtD., is shown in TABLE 1. Unmodified AlZn10Si8Mg alloy (UNIFONT® – 90) has very good casting properties, good wear resistance, low thermal expansion, and very good machining. The alloy contains relatively high Si content, and impurity limits tend to be relatively loose. The only intentional and controlled additions of Zn to Al-casting alloys are currently commonly used in the 7XXX series, but these alloys are not yet suitable for die casting. Otherwise, Zn is present only as an acceptable impurity element in many secondary (scrap-based) Al-cast alloys for die casting. As Zn is considered quite neutral it neither enhances nor detracts from an alloy's properties. It should be recognized that Zn is a relatively dense (heavy) element, and as such, it increases an alloy's mass density. On the other hand, alloys of the 4XXX group (Al-Zn-Si-Mg), also referred to as zinc silumines, appear to be suitable for die casting. These, though having many advantages, are only used to a very limited extent. Zinc as an addition in Al-Si alloys is of special importance, does not interact with other constituents in small quantities, and does not have any practical effect on the mechanical properties of the alloy [17,18].

High-zinc secondary alloys usually seem attractive due to the cost slightly less than low-zinc alloys. However, this attractiveness can be misleading if the difference in cost is too small; buying cheaper alloys may make little sense if it means that more weight of the material is being transported with each casting [19,20]. AlZn10Si8Mg cast alloy is a self-hardening alloy that is particularly used when good strength values are required without the need for heat treatment. With these alloy types, the mechanical properties are achieved after storage of approximately 7 to 10 days at room temperature. Particular attention should

TABLE 1

Chemical composition of experimental alloys [wt. %]

Alloys	Si	Zn	Mg	Fe	Cu	Mn	Ti	Sb	Ni	Sn	Al
AlSi7Mg0.3	7.03	—	0.35	0.12	0.013	0.009	0.123	0.007	—	0.004	Bal.
AlSi7Mg0.3+T6	7.34	—	0.32	0.13	0.012	0.034	0.109	0.007	—	0.004	Bal.
AlZn10Si7Mg	8.64	9.6	0.45	0.12	0.005	0.181	0.062	—	0.002	—	Bal.

be paid to the high 0.2% yield strength. The low iron content has a particularly beneficial effect on the mechanical properties, which can also be traced to good fatigue strength [19,20].

3. Experimental procedure

Cast samples were sectioned from the test bars (in transversal and longitudinal directions). The samples (1.5×1.5 cm) were mechanically ground, polished, and standard prepared for metallographic observations. The microstructures were studied using a light optical microscope Neophot 32. Samples were etched by standard reagent HF. A few samples were also deep-etched for 30 s in HCl solution in order to reveal the three-dimensional morphology of the silicon phase. The specimen preparation procedure for deep-etching consists of dissolving the aluminum matrix in a reagent that will not attack the eutectic silicon or intermetallic phases [21,22]. The various phases reported in this work were identified using a scanning electron microscope VEGA LMU II connected to the energy-dispersive X-ray spectroscopy with EDX analyzer Brucker Quantax. All phases were analyzed by the EDX mapping technique.

After metallographic evaluation, the Brinell hardness test (STN EN ISO 6506-1) was performed on the experimental alloys. For measuring were used parameters: load at 2451.66 N (250 Kp), dwell ball with a diameter of 5 mm, and time 15 s. The micro Vickers hardness was measured in HTW Dresden using an MHT-1 microhardness tester under a 0.009 (1g) N load for 10 s. (HV 0.01). The evaluated HBW and HV0.01 reflect average values of at least ten separately experimental specimens.

The fatigue lifetime of experimental alloys was measured on 15 test specimens required to determine S-N curves according to the STN EN ISO 1143:2021 standard with dimensions documented in Fig. 1. All specimens were longitudinally polished to eliminate circumferential machining. The tests were performed on an experimental device for rotation-bending fatigue testing with different strain rates with a loading frequency = 30 Hz, a load ratio of $R = -1$ at room temperature $T = 22\pm1$°C. Fatigue testing was established on regime σ_c at $N = 5\times10^6$ cycles to failure a request from UNEKO, LtD. [23].

The tensile tests, three specimens for each alloy, were carried out at room temperature on test machine INSTRON Model 5985 according to the standard ISO 6892-1:2009. Test rates and controls were set according to Method A recommended range [24]. Yield strength (YS), ultimate tensile strength (UTS), and elongation to failure (A) were measured. The evaluated UTS, YS, and A reflect average values of at least six separate bars.

4. Results

4.1. Microstructure comparison

The representative microstructures of experimental materials are documented in Fig. 2. The typical microstructure of secondary AlZn10Si8Mg cast alloy (Fig. 2a) consists of α(Al)-matrix, eutectic (E), and various types of intermetallic phases. The α-matrix precipitates from the liquid as the primary phase in the form of dendrites and nominally consists of Al and Zn [21]. The microstructure of AlSi7Mg0.3 cast alloys (Fig. 2b,c) is given by a binary Al-Si phase diagram and consists of α(Al)-matrix, eutectic (E), and intermetallic phases primarily based on Fe as a result of the scrap-recycling process.

During solidification, a variety of intermetallic particles formed in the commercial 7xxx class aluminum alloys. Metals such as Mg, Fe, Mn, and Cu are common in this Al-alloy in addition to the intentionally added elements. These impurities, even in small amounts, lead to the formation of a new phase component [21]. In the microstructure of AlZn10Si8Mg were additionally observed 2 types of intermetallic compounds oval round-like particles – Al_2CuMg and ternary eutectic – Al-$MgZn_2$-Cu compared to AlSi7Mg0.3 cast alloys. SEM observation combined with EDX mapping analysis was used for the identification of phases, documented in Fig. 3.

As the basic intermetallic phase present in all alloys is Mg_2Si in the form of a Chinese script. Mg-rich phases in Al-Zn-Si alloy solidify in two different forms as Mg_2Si and Al_2CuMg detected as S-phase (Fig. 3a) [21]. In the microstructure of AlZn10Si8Mg, this phase is present in a higher amount and is larger in size compared to AlSi7Mg0.3 cast alloys. The other phases identified in all experimental alloys were Fe-rich phases as: AlFeMnMgSi/AlFe(Mn)Ni phase, most frequently in the shape of Chinese script and the Al_5FeSi phase with the typical needle-like morphology (Fig. 4). In particular, the platelet/needle-like morphology is considered to be the most detrimental to mechanical properties, promoting the formation of casting defects, such as porosity and shrinkage [2,21,23].

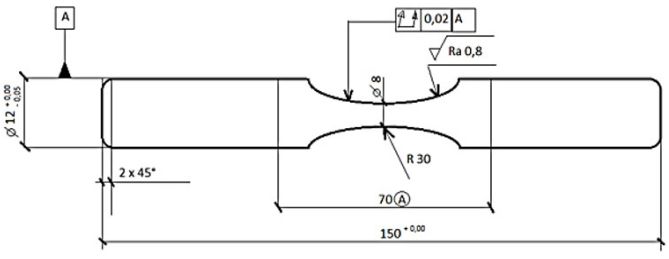

a) fatigue test

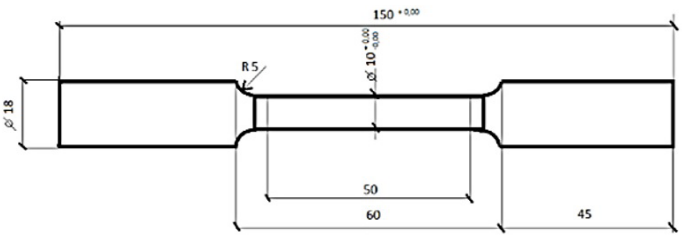

b) tensile test

Fig. 1. Shape and dimensions (mm) of the experimental specimens

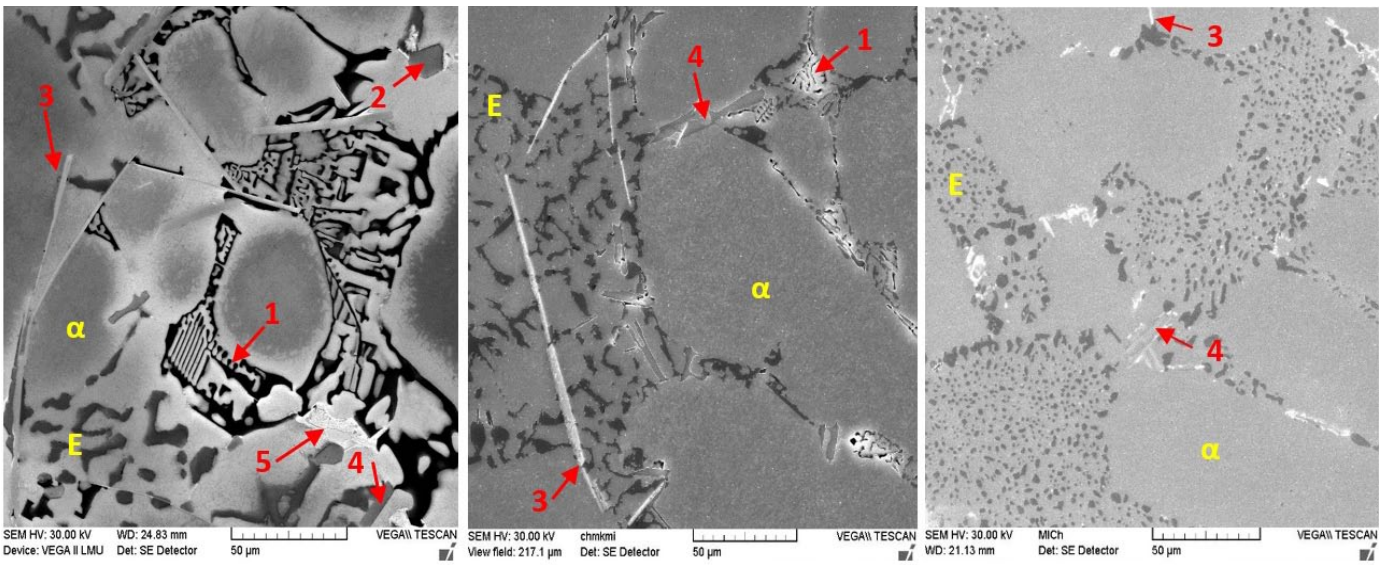

a) AlZn10Si8Mg b) AlSi7Mg0.3 c) AlSi7Mg0.3 + T6

Fig. 2. Microstructure of experimental alloys: 1 – Mg_2Si, 2 – Al_2CuMg, 3 – Al_5FeSi, 4 – AlFeMnMgSi/ AlFe(Mn)Ni, 5 – ternary eutectic Al-$MgZn_2$-Cu; etch. 0.5% HF, SEM

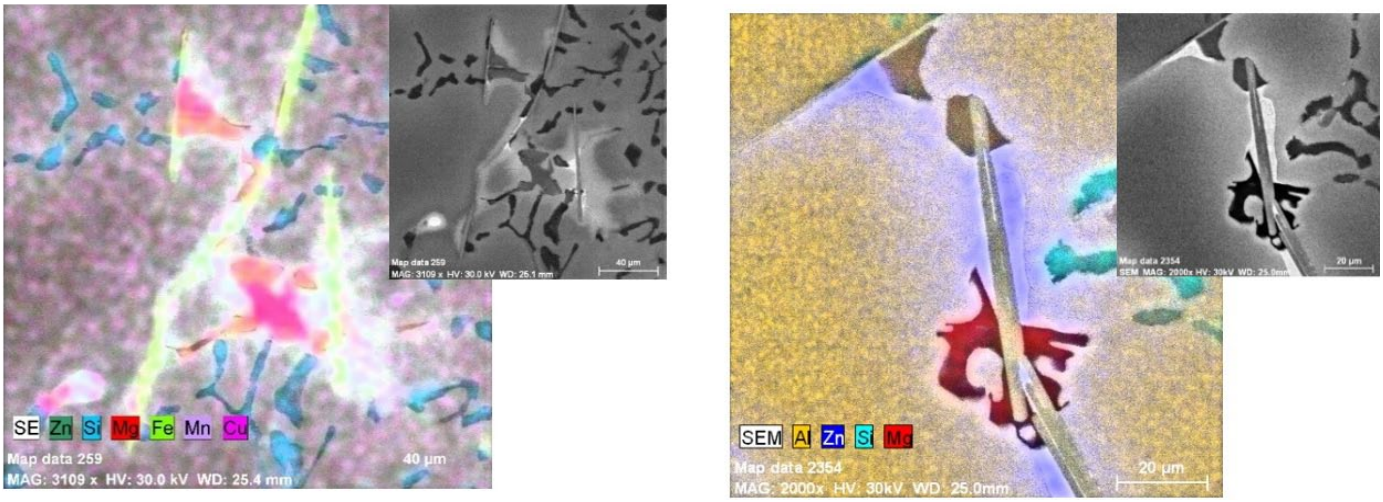

a) oval round-like particles Al_2CuMg b) ternary eutectic Al-$MgZn_2$-Cu

Fig. 3. EDX analysis of additional intermetallic phases in AlZn10Si8Mg alloy; etch.0.5% HF, SEM

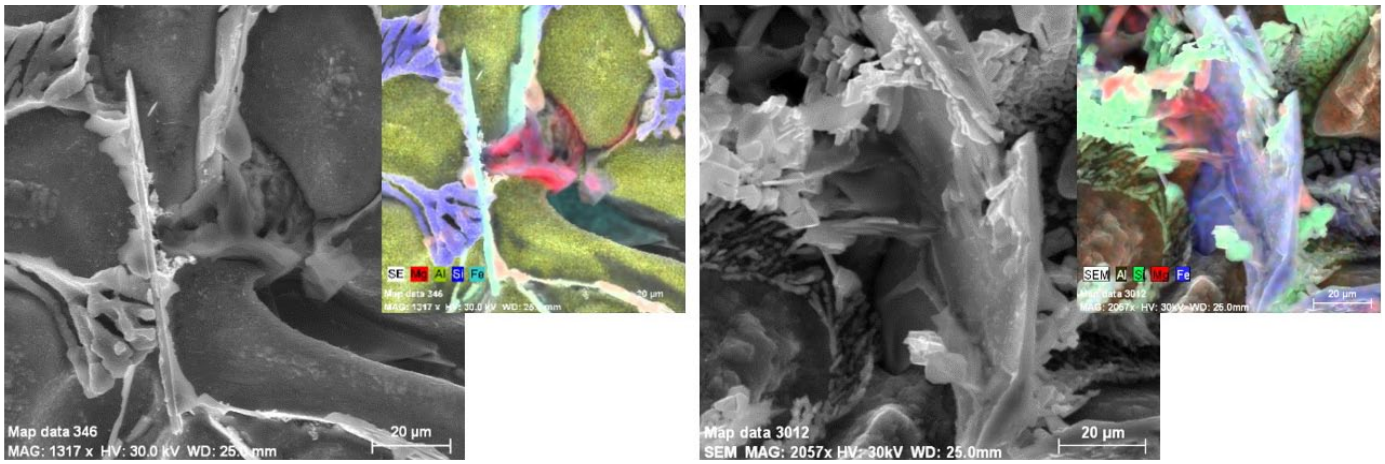

a) AlZn10Si8Mg b) AlSi7Mg0.3

Fig. 4. Morphology of needle-like Fe-rich phase of experimental alloys; deep-etch. HCl, SEM

The last intermetallic phase common to all experimental alloys is in the form of sharp-edge particles for AlZn10Si8Mg is identified as AlFeMnMgSi or Al(FeMn)Ni and for AlSi7Mg0.3 alloys is identified as AlFeMnMgSi or Al(FeMn)Si. From a morphological point of view in Fig. 5, can be observed that these sharp-edged particles are much smaller for AlZn10Si7Mg alloy compared to AlSi7Mg0.3 alloys.

In addition to metallographic observation, deep etching methods were used for a comparison of the 3D morphology of eutectic silicon as well (Fig. 6). Eutectic silicon in AlZn10Si8Mg alloy exhibits as a rosette-like, rather than brittle plate-like form (Fig. 6a). The center of the rosette is probably the center of the eutectic grain, which indicates that the nucleation of eutectic phases independently of the surrounding primary α-Al dendrites. The morphology of eutectic silicon in AlSi7Mg0.3 alloy is similar (Fig. 6b), Si is observed as fine sticks growing in clusters from a single nucleation site. After T6 heat treatment, significant spheroidization of the eutectic silicon was achieved, whose 3D morphologies are small, isolated round particles [21,22].

4.2. Results of mechanical tests

The results from tensile and hardness testing of experimental alloys are shown in TABLE 2 and documented in Fig. 7. From the overall results, it can be concluded that the AlSi7Mg0.3+T6 alloy obtained the best mechanical properties except for yield strength. Comparing the YS of AlZn10Si8Mg alloy with AlSiMg0.3 (T6), this alloy shows on average approximately 17 MPa higher YS. This difference in YS probably may be attributed to the larger and coarser Si particles. The Si-particles are expected to have a significantly higher yield strength because they are significantly harder than the matrix. A microhardness value of 155 HV 0.01 was measured for the eutecticum com-

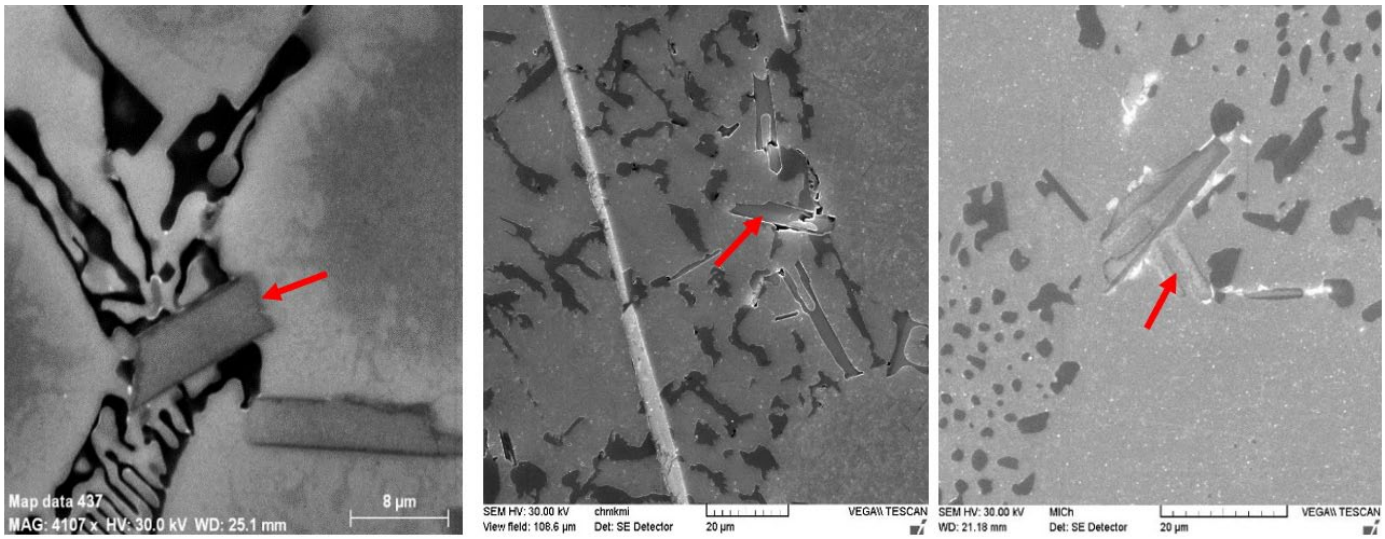

a) AlZn10Si8Mg b) AlSi7Mg0.3 c) AlSi7Mg0.3 + T6

Fig. 5. Morphology of sharp-edged particles of Fe-rich phases; deep-etch. HCl, SEM

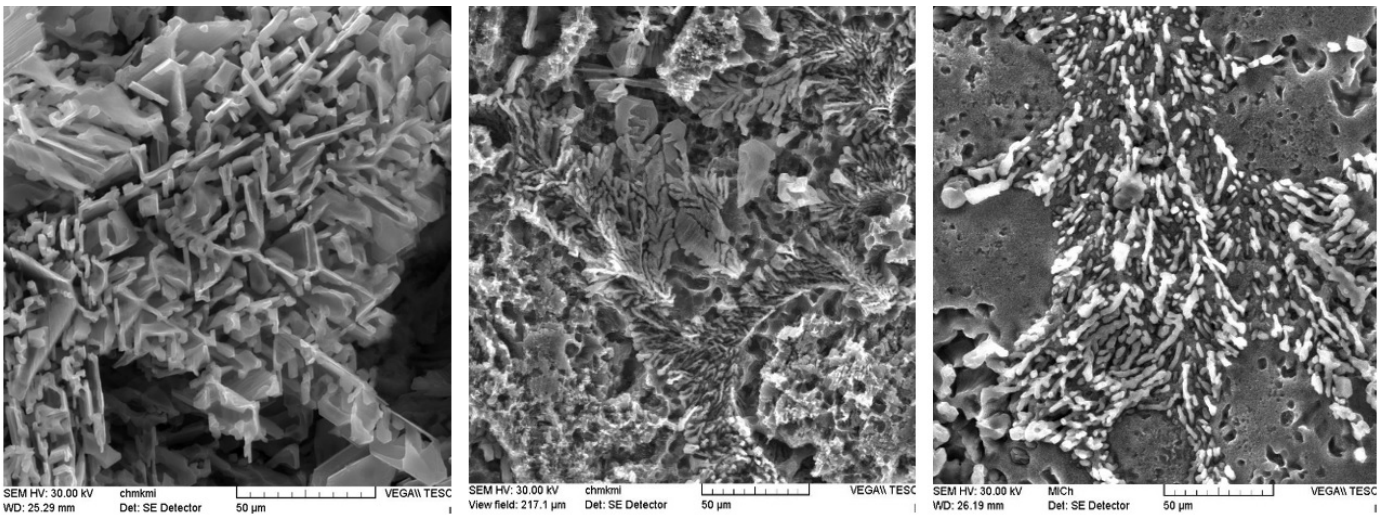

a) AlZn10Si8Mg b) AlSi7Mg0.3 c) AlSi7Mg0.3+T6

Fig. 6. Morphology of Si particles of experimental alloys, deep-etch. HCl, SEM

TABLE 2

Mechanical properties of experimental alloys

Alloy	UTS [MPa]	YS [MPa]	A [%]	HBW 5/250/15	HV0.01 α-matrix	HV0.01 eutectic
AlSi7Mg0.3	144±4	100.9±2	1.5±0.5	54.8±2	54.3±2	65.0±10
AlSi7Mg0.3+T6	218±10	168.3±10	2.5±0.6	93.2±2	94.6±2	112.7±25
AlZn10Si8Mg	187±7	185.0±7	2.0±0.5	83.0±0	92.0±1	155.0±20

pared to the aluminum matrix with a hardness value of 92 HV 0.01. The higher yield strength of the AlSiMg0.3 (T6) alloy compared to the AlSi7Mg0.3 alloy in the as-cast state is due to the expected effect of precipitation hardening. Precipitation hardening leads to a gradual increase in YS, hardness, and α-matrix microhardness due to precipitate Mg_2Si particles of the low-temperature phase inhibiting the movement of dislocations/defects in the lattice structure of AlSi7Mg0.3 alloy. The lower elongations measured in the AlZn10Si8Mg samples are mainly due to the coarser Si particles compared to the AlSi7Mg0.3+T6 alloy. Hardness and microhardness measurements both indicate that the higher hardness of the materials after T6 heat treatment is related to the formation of Mg_2Si precipitates in the substructure of the experimental AlSi7Mg0.3 alloys [11]. Therefore, the lowest values and thus the worst results are achieved by the AlSi7Mg0.3 alloy in the as-cast condition. AlZn10Si8Mg alloy has lower but still comparable tensile properties to AlSi7Mg0.3+T6 alloy. These values are suitable for castings in the automotive industry.

4.3. Results of fatigue tests

The obtained results of fatigue tests are illustrated in Fig. 8. The fatigue properties of cast aluminium alloy are significantly affected by structural inhomogeneity, higher iron content, and the presence of casting defects such as porosity as reported by Kuchariková [11] and Samuel [25]. The fatigue strength is slightly affected by chemical composition, heat treatment, or solidification time [21,22]. From the measured S-N curve, it can be observed clearly that the fatigue life increases with decreasing stress amplitude, and the S-N curve seems to decrease continuously with increasing lifetime. The lowest fatigue lifetime has AlSi7Mg0.3 alloy in the as-cast condition. On the other hand, the best and at the same time almost identical fatigue lifetime was achieved by AlSi7Mg0.3+T6 with AlZn10Si8Mg alloy as the result of fine precipitates of Mg_2Si phase inside the α-matrix ensuring the effective strengthening of the alloy with a high modulus of elasticity [26,27]. By statistical calculations from the measured S-N curves were established the Basquin equation: $\sigma_a = \sigma'_f (2N_f)^b$, where σ_a is the stress amplitude, σ'_f is the fatigue strength coefficient, defined as the stress intercept at $2N = 1$.σ'_f is approximately equal to the true fracture stress, b is the fatigue strength (also known as Basquin) exponent and $2N_f$ is the reversals to failure. Basquin's equation is a power-law relationship that describes the linear relationship between the applied stress cycles (S) on the y-axis and the number of cycles to failure on the x-axis plotted on a log-log scale [11]. The possibility to create and use the Basquin Equations (1)-(3) for the prediction of fatigue life for the different number of cycles shows that the order is different under a lower stress amplitude: for (1), (2), and (3) with the aim to predict the fatigue life for different stress amplitudes:

AlSi7Mg0.3 alloy in as-cast state:

$$\sigma_a = 2274.6 \times N_f^{-0,246} \quad (1)$$

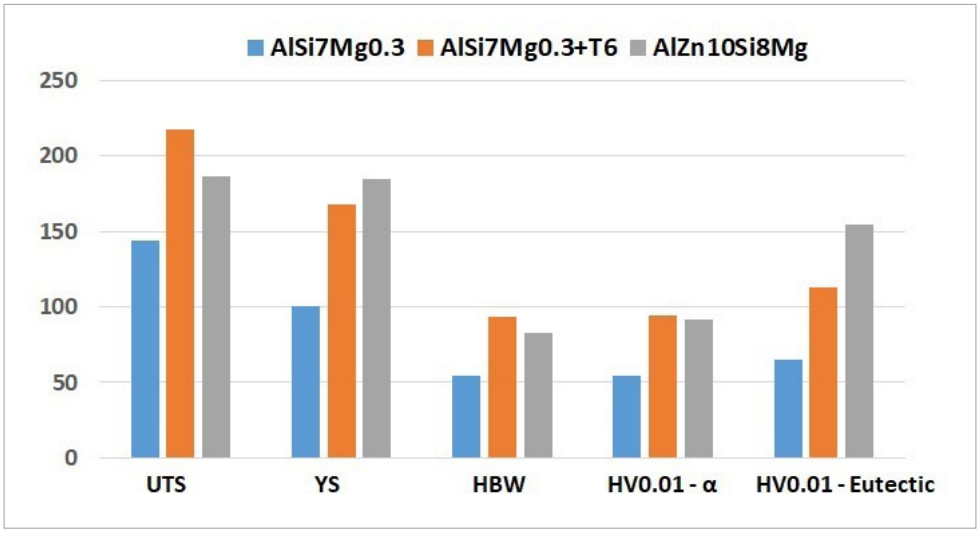

Fig. 7. Mechanical tests results of experimental alloys

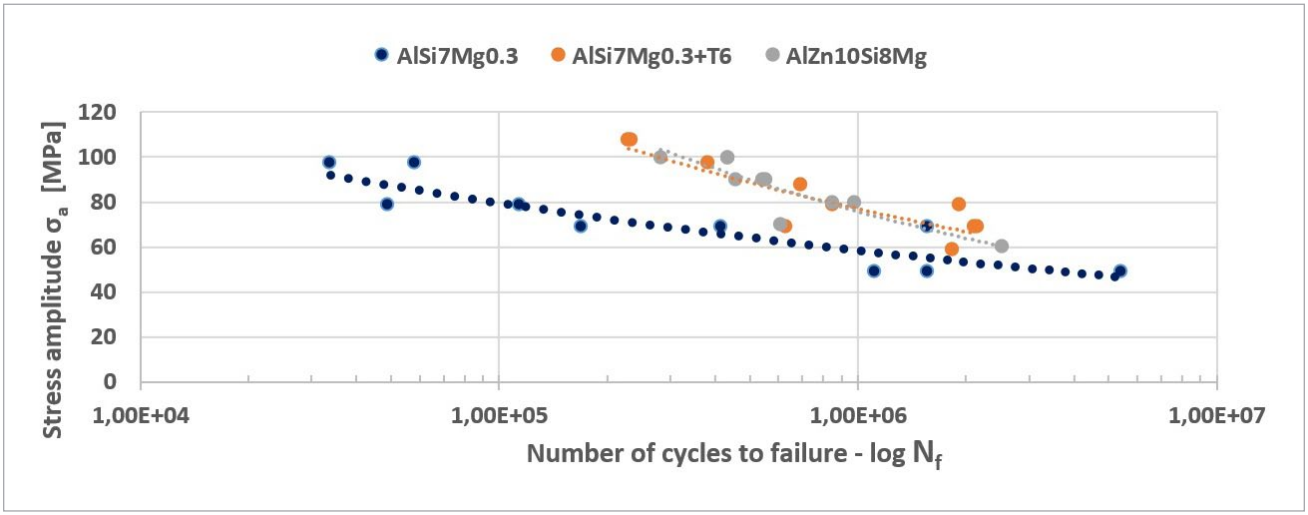

Fig. 8. The S-N curves

AlSi7Mg0.3 + T6:

$$\sigma_a = 1284.1 \times N_f^{-0,204} \quad (2)$$

AlZn10Si8Mg alloy:

$$\sigma_a = 372.02 \times N_f^{-0,134} \quad (3)$$

5. Conclusion

All experimental alloys have comparable main structural components. The microstructure consists of α-phase, eutectic and intermetallic phases. The amount and chemical composition of intermetallic phases depend on the type of experimental alloy, but all of them contain Chinese script – Mg_2Si, Fe-needle-like (Al_5FeSi) phases, and Sharp-edged particles. The self-hardened alloy additionally contains oval round-like particles – Al_2CuMg and ternary eutectic – Al-$MgZn_2$-Cu.

The morphology of eutectic silicon AlSi7Mg0.3 alloy (as-cast state) is comparable with self-hardened AlZn10Si8Mg alloy, but silicon is finer. Eutectic silicon after heat treatment (AlSi7Mg0.3+T6) spheroidized and is in the form of isolated round particles.

The results of mechanical properties show that experimental material AlSi7Mg0.3+T6 has the best properties, but the differences with the self-hardened alloy are small:

- the AlSi7Mg0.3+T6 cast alloy has of about 14% higher UTS, 10% HBW, 3% HV 0.01 α-matrix, 2.5% ductility,
- the AlZn10Si8Mg alloy has up to 10% higher YS and about 37% higher HV 0.01 eutectic.

The results of fatigue properties of AlSi7Mg0.3 alloy show that the heat treatment significantly increases fatigue lifetime. The fatigue curve shifts to the right, i.e. at the same load the experimental AlSi7Mg0.3 alloy sustains a higher number of cycles to fracture. The AlZn10Si8Mg alloy has the same fatigue lifetime as AlSi7Mg0.3+T6 alloy at all measured stress amplitude.

The results of this study confirmed that self-hardened AlZn10Si8Mg cast alloys can replace commonly used AlSi7Mg cast alloys in the future. The use of these alloys for the production of mechanical components used in the automotive industry will offer significant economic and environmental benefits, thanks to the possibility of eliminating heat treatment.

Acknowledgement

The research was supported by Scientific Grand Agency of Ministry of Education of Slovak Republic and Slovak Academy of Sciences, VEGA 01/0398/19, KEGA 016ŽU-4/2020, project to support young researches at UNIZA, ID project 12715 and project 313011ASY4 "Strategic implementation of additive technologies to strengthen the intervention capacities of emergencies caused by the COVID-19 pandemic".

REFERENCES

[1] https://european-aluminium.eu/resource-hub/recycling-aluminium-a-pathway-to-a-sustainable-economy/, accessed: 10.06.2022

[2] D. Závodská, et al., Effects of Porosity on the Fatigue Behaviour of AlZn10Si8Mg Casting Alloys in a High Cycle Region, in: A. Sedmak, Z. Radaković, M. Rakin (EDS), Procedia Engineering 2017, Loading and Environmental effects on Structural Integrity (2017).

[3] https://recycling.world-aluminum.org/fileadmin/_migrated/content_uploads/fl0000217_04.pdf, accessed: 11.06.2022

[4] B. Zhou, B. Liu, S. Zhang, R. Lin, Y. Jiang, X. Lan, Journal of Alloys and Compounds **879**, 160407 (2021).

[5] J. Svobodova, et al., Manufacturing Technology **19** (6), 1041-1046 (2019).

[6] D. Song et al., Materials **15**, 1618 (2022).

[7] L. Kuchariková, et al., Analysis of microstructure in AlSi7Mg0.3 cast alloy with different content of Fe, in: J. Bujňák, M. Guagliano (EDS) Transport research procedia 2019, TRANSCOM 2019 13th International Scientific Conference on Sustainable, Modern and Safe Transport (2019).

[8] C.R. Barbosa, et al., Met. Mater. **26**, 370-383 (2020).
[9] Peter et al., 2020 IOP Conf. Ser.: Mater. Sci. Eng. 916 012082
[10] D. Khoukhi, et al., Probabilistic modeling of the size effect and scatter in High Cycle Fatigue using a Monte-Carlo approach: Role of the defect population in cast aluminum alloys, International Journal of Fatigue **147**, 106177 (2021).
[11] L. Kuchariková, et al., Investigation on microstructural and hardness evaluation in heat-treated and as-cast state of secondary AlSiMg cast alloys, in: R. Zemčík (EDS), Materials Today: Proceedings 2020, DAS 2019 (2020).
[12] E. Kantoríková, et al., Archives of Foundry Engineering **21** (2), 89-93 (2021).
[13] W. Kim, et al., Appl. Sci. **11** (23), 11572 (2021).
[14] A. Isadare, et al., Materials Research **16** (1), 190-194 (2013).
[15] M. Rosso, et al., Metals and Materials Society. Light Metals 213-218 (2014).
[16] M. Vicen, Archives of Foundry Engineering **17** (3), 139-142 (2017).
[17] J. Pezda, Archives of Foundry Engineering **12** (2), 135-138 (2012).
[18] E. Czekaj, H. Dybiec, A. Fajkiel, P. Sadowski, Casting Zinc Silumins – Odlewnicze siluminy cynkowe. (2011).
[19] X. Yu, L. Wang, T6 heat-treated AlSi10Mg alloys additive-manufactured by selective laser melting, in: K. Mori, Y. Abe, T. Maeno (EDS), Procedia Manufacturing 2018, Proceedings of the 17th International Conference on Metal Forming Metal Forming 2018 (2018).
[20] Y. Liu, et al., Journal of Materials Research and Technology **14**, 2571-2578 (2021).
[21] E. Tillová, et al., Acta Metallurgica Slovaca **17** (1), 4-10 (2011).
[22] E. Tillová, M. Chalupová, Acta metallurgica Slovaca **1**, 847-849 (2004).
[23] L. Kuchariková, et al., Materials **14**, 1943 (2021).
[24] L. Kuchariková, et al., Investigation of mechanical properties of secondary AlSi7Mg0.3 cast alloys before and after corrosion, in: IOP Conference Series: Materials Science and Engineering 2020, 6th International Conference on Recent Trends in Structural Materials (COMAT 2020) 30th November – 4th December 2020, Pilsen, Czech Republic (2020).
[25] A.M. Samuel, Met. Mater. Trans. A **26**, 2359-2372 (1995).
[26] W. Chao, et al., High Temperature Materials and Processes **37** (4), 289-298 (2018).
[27] X. Jiang, et al., Transactions of Nonferrous Metals Society of China **21**, 443-448 (2011).